Cell

A Common Mechanism of Cellular Death Induced by Bactericidal Antibiotics

Michael A. Kohanski,[1,2,5,6] Daniel J. Dwyer,[1,3,6] Boris Hayete,[1,4] Carolyn A. Lawrence,[1,2] and James J. Collins[1,2,3,4,*]
[1] Center for BioDynamics and Center for Advanced Biotechnology
[2] Department of Biomedical Engineering
[3] Program in Molecular Biology, Cell Biology, and Biochemistry
[4] Bioinformatics Program
Boston University, Boston, MA 02215, USA
[5] Boston University School of Medicine, Boston, MA 02118, USA
[6] These authors contributed equally to this work.
*Correspondence: jcollins@bu.edu
DOI 10.1016/j.cell.2007.06.049

SUMMARY

Antibiotic mode-of-action classification is based upon drug-target interaction and whether the resultant inhibition of cellular function is lethal to bacteria. Here we show that the three major classes of bactericidal antibiotics, regardless of drug-target interaction, stimulate the production of highly deleterious hydroxyl radicals in Gram-negative and Gram-positive bacteria, which ultimately contribute to cell death. We also show, in contrast, that bacteriostatic drugs do not produce hydroxyl radicals. We demonstrate that the mechanism of hydroxyl radical formation induced by bactericidal antibiotics is the end product of an oxidative damage cellular death pathway involving the tricarboxylic acid cycle, a transient depletion of NADH, destabilization of iron-sulfur clusters, and stimulation of the Fenton reaction. Our results suggest that all three major classes of bactericidal drugs can be potentiated by targeting bacterial systems that remediate hydroxyl radical damage, including proteins involved in triggering the DNA damage response, e.g., RecA.

INTRODUCTION

Current antimicrobial therapies, which cover a wide array of targets (Walsh, 2003), fall into two general categories: bactericidal drugs, which kill bacteria with an efficiency of >99.9%, and bacteriostatic drugs, which merely inhibit growth (Pankey and Sabath, 2004). Antibacterial drug-target interactions are well studied and predominantly fall into three classes: inhibition of DNA replication and repair, inhibition of protein synthesis, and inhibition of cell-wall turnover (Walsh, 2000). The bactericidal antibiotic killing mechanisms are currently attributed to the class-specific drug-target interactions. However, our understanding of many of the bacterial responses that occur as a consequence of the primary drug-target interaction remains incomplete (Davis, 1987; Drlica and Zhao, 1997; Lewis, 2000; Tomasz, 1979).

Bacteriostatic drugs predominantly inhibit ribosome function, targeting both the 30S (tetracycline family and aminocyclitol family) and 50S (macrolide family and chloramphenicol) ribosome subunits (Chopra and Roberts, 2001; Poehlsgaard and Douthwaite, 2005; Tenson et al., 2003; Weisblum and Davies, 1968). The aminocyclitol group of 30S inhibitors includes the bactericidal aminoglycoside family of drugs and the bacteriostatic drug spectinomycin; the aminoglycoside family, excluding spectinomycin, is the only class of ribosome inhibitors known to cause protein mistranslation (Davis, 1987; Weisblum and Davies, 1968). With regard to other classes of bactericidal antibiotics, quinolones target DNA replication and repair by binding DNA gyrase complexed with DNA, which drives double-strand DNA break formation and cell death (Drlica and Zhao, 1997). Cell-wall synthesis inhibitors (such as β-lactams), which interact with penicillin-binding proteins (Tomasz, 1979) and glycopeptides that interact with peptidoglycan building blocks (Reynolds, 1989), interfere with normal cell-wall synthesis and induce lysis and cell death. With the alarming spread of antibiotic-resistant strains of bacteria (Walsh, 2000, 2003), a better understanding of the specific sequence of events leading to cell death from the wide range of bactericidal antibiotics is needed for future antibacterial drug advancement.

We have recently shown that bacterial gyrase inhibitors, including synthetic quinolone antibiotics and the native proteic toxin CcdB, induce a breakdown in iron regulatory dynamics, which promotes formation of reactive oxygen species that contribute to cell death (Dwyer et al., 2007). Hydroxyl radical formation utilizing internal iron and the Fenton reaction appears to be the most significant contributor to cell death among the reactive oxygen species formed. The Fenton reaction leads to the formation of

hydroxyl radicals through the reduction of hydrogen peroxide by ferrous iron (Imlay et al., 1988; Imlay and Linn, 1986). We chose to investigate whether hydroxyl radical formation also contributes to antibiotic-induced cell death in bacteria among the other classes of antibiotics. Here we report that the three major classes of bactericidal antibiotics, regardless of drug-target interaction, stimulate hydroxyl radical formation in bacteria. Furthermore, we demonstrate that hydroxyl radical generation contributes to the killing efficiency of these lethal drugs. We also show, in contrast, that bacteriostatic drugs do not produce hydroxyl radicals. We demonstrate that all bactericidal drug classes utilize internal iron from iron-sulfur clusters to promote Fenton-mediated hydroxyl radical formation and show that these events appear to be mediated by the tricarboxylic acid (TCA) cycle and a transient depletion of NADH. We propose that there is a common mechanism of cellular death underlying all classes of bactericidal antibiotics whereby harmful hydroxyl radicals are formed as a function of metabolism-related NADH depletion, leaching of iron from iron-sulfur clusters, and stimulation of the Fenton reaction.

RESULTS

Bactericidal Antibiotics Induce Hydroxyl Radical Formation

Using the dye hydroxyphenyl fluorescein (HPF), which is oxidized by hydroxyl radicals with high specificity (Setsukinai et al., 2003), we first examined a concentration of hydrogen peroxide known to induce hydroxyl radical formation via Fenton chemistry (Imlay et al., 1988). As expected (Imlay et al., 1988), we observed cellular death with 1 mM hydrogen peroxide (Figure 1A) accompanied by an increase in HPF fluorescence (Figure 1B). Additionally, we confirmed dye specificity for hydroxyl radicals by inhibiting the Fenton reaction and hydroxyl radical formation with the iron chelator 2,2′-dipyridyl and by directly quenching Fenton-generated hydroxyl radicals with the hydroxyl radical scavenger thiourea (Figures 1A and 1B). Application of iron chelators is an established means of blocking Fenton reaction-mediated hydroxyl radical formation by sequestering unbound iron (Imlay et al., 1988). Thiourea is a potent hydroxyl radical scavenger that is an established means of mitigating the effects of hydroxyl radical damage in both eukaryotes and prokaryotes (Novogrodsky et al., 1982; Repine et al., 1981; Touati et al., 1995). In this manner, we showed that HPF fluorescence is a reliable measure of hydroxyl radical formation in bacteria.

We next investigated hydroxyl radical formation following exposure to the three major classes of bactericidal antibiotics in *Escherichia coli* (*E. coli*) (Figures 1C and 1D). Specifically, we examined killing by the quinolone (250 ng/ml norfloxacin), β-lactam (5 μg/ml ampicillin), and aminoglycoside (5 μg/ml kanamycin) classes. We found that each of the three different classes of bactericidal antibiotics induced hydroxyl radical formation (Figure 1D); norfloxacin and ampicillin induced hydroxyl radical formation within 1 hr and kanamycin by 2 hr after addition of drug (see Figure S1 in the Supplemental Data available with this article online). In contrast, the five bacteriostatic drugs we tested (Figure 1E), including four different classes of ribosome inhibitors (chloramphenicol, spectinomycin, tetracycline, and the macrolide erythromycin) as well as an inhibitor of RNA polymerase (rifamycin SV, referred to as rifamycin; Wehrli and Staehelin [1971]), did not stimulate hydroxyl radical production (Figure 1F and Figure S2D).

Interestingly, in ampicillin-treated cultures, we observed a bimodal distribution of hydroxyl radical production at 2 and 3 hr post drug application (Figure 1D and Figure S1C) that correlated with the onset of cell lysis (Figure S8A); the decline in the number of cells producing radicals between 2 and 3 hr is consistent with the ongoing cell lysis. In contrast, prior to lysis (1 hr posttreatment), ampicillin application yielded a uniform increase in hydroxyl radical formation (Figures S1C and S8A). These results suggest a role for hydroxyl radicals in both the lethal and lytic effects of β-lactams.

We sought to demonstrate that Gram-positive, as well as Gram-negative, bacteria produce hydroxyl radicals in response to bactericidal antibiotics. We examined hydroxyl radical production for a bacteriostatic drug (chloramphenicol), a bactericidal drug (norfloxacin), and both lethal (5 μg/ml) and sublethal (1 μg/ml) concentrations of vancomycin (a Gram-positive specific bactericidal drug; Reynolds [1989]) in a wild-type strain of *Staphylococcus aureus* (*S. aureus*) (Figure S3A). We observed an increase in hydroxyl radical production for the norfloxacin treatment and for the lethal concentration of vancomycin (Figure S3). Conversely, we did not observe hydroxyl radical production for the chloramphenicol treatment or the sublethal concentration of vancomycin, the latter of which had no effect on growth (Figure S3). Cumulatively, our hydroxyl radical results suggest that the genetic and biochemical changes that arise following application of lethal doses of bactericidal antibiotics create an intracellular environment that promotes the formation of highly deleterious oxidative radical species.

Hydroxyl Radical Formation for All Bactericidal Classes Involves the Fenton Reaction and Intracellular Iron

To demonstrate that hydroxyl radical formation is an important component of norfloxacin-, ampicillin-, and kanamycin-mediated killing, we additionally treated drug-exposed wild-type *E. coli* with the iron chelator 2,2′-dipyridyl. For the three classes of bactericidal drug treatments, we observed a significant increase in bacterial survival following addition of 2,2′-dipyridyl (Figures 2A, 2C, and 2E), confirming that hydroxyl radicals are involved in bactericidal antibiotic-induced cell death. 2,2′-dipyridyl significantly reduced hydroxyl radical formation in norfloxacin-treated cultures (Figure 2B), and there appeared to

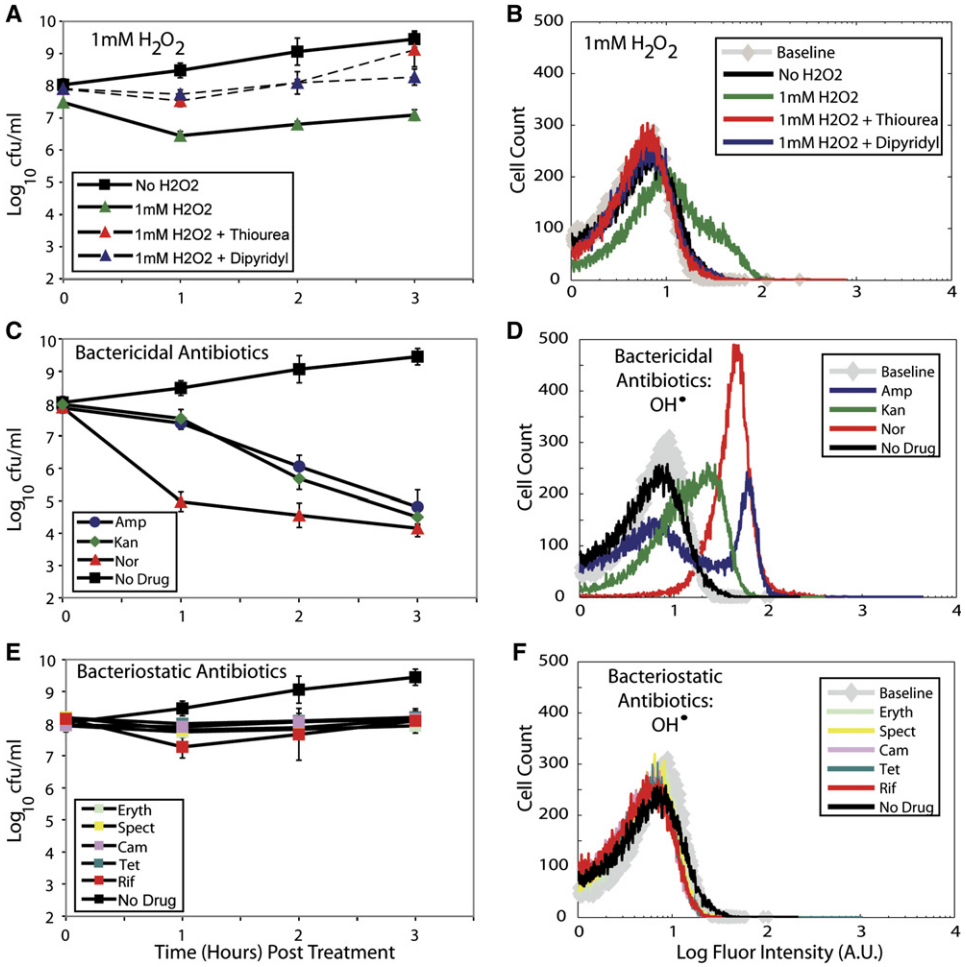

Figure 1. Hydroxyl Radical Production in *E. coli* by Hydrogen Peroxide and Antibiotics

(A, C, and E) Log change in colony-forming units per milliliter (cfu/ml). Black squares represent a no-drug control. In this and all other figures, error bars represent ±SD of the mean.

(B, D, and F) Generation of hydroxyl radicals. Representative measurements are shown and were taken 3 hr following addition of drug. Gray diamonds represent time-zero baseline measurements.

(A and B) Survival (A) and hydroxyl radical formation (B) following 1 mM H_2O_2 treatment alone (green), plus 150 mM thiourea (red), or plus 500 μM 2, 2′-dipyridyl (blue).

(C and D) Survival (C) and hydroxyl radical generation (D) following exposure to bactericidal antibiotics (5 μg/ml ampicillin [Amp], blue; 5 μg/ml kanamycin [Kan], green; 250 ng/ml norfloxacin [Nor], red).

(E and F) Survival (E) and hydroxyl radical generation (F) following exposure to bacteriostatic drugs (600 μg/ml erythromycin [Eryth], light blue; 400 μg/ml spectinomycin [Spect], yellow; 15 μg/ml chloramphenicol [Cam], pink; 10 μg/ml tetracycline [Tet], blue; 500 μg/ml rifamycin [Rif], red).

be some recovery from the norfloxacin-induced growth arrest and DNA damage between 2 and 3 hr into the treatment in the presence of 2,2′-dipyridyl (Figure 2A). Similarly, killing by ampicillin and kanamycin was reduced to less than 0.5 logs following application of the iron chelator (Figures 2C and 2E) and was accompanied by a significant reduction in hydroxyl radical formation (Figures 2D and 2F). As expected, addition of the iron chelator to bacteriostatic drug-treated cultures, which do not produce hydroxyl radicals, had no effect on the growth-arresting properties of these bacteriostatic classes of drugs (Figure S4A).

We next sought to directly block the harmful effects of hydroxyl radicals generated via the Fenton reaction by adding thiourea to drug-treated cultures. We found that cultures treated with norfloxacin and thiourea showed a significant delay in cell death at 1 hr and a near 1-log increase in survival at 3 hr relative to norfloxacin treatment alone (Figure 2A). This increase in survival again correlated with a decrease in the detectable levels of hydroxyl radicals (Figure 2B). Thiourea was able to reduce ampicillin-mediated killing (Figure 2C) and hydroxyl radical formation (Figure 2D) to the same extent that 2,2′-dipyridyl was. Thiourea was less efficient at mitigating bacterial cell

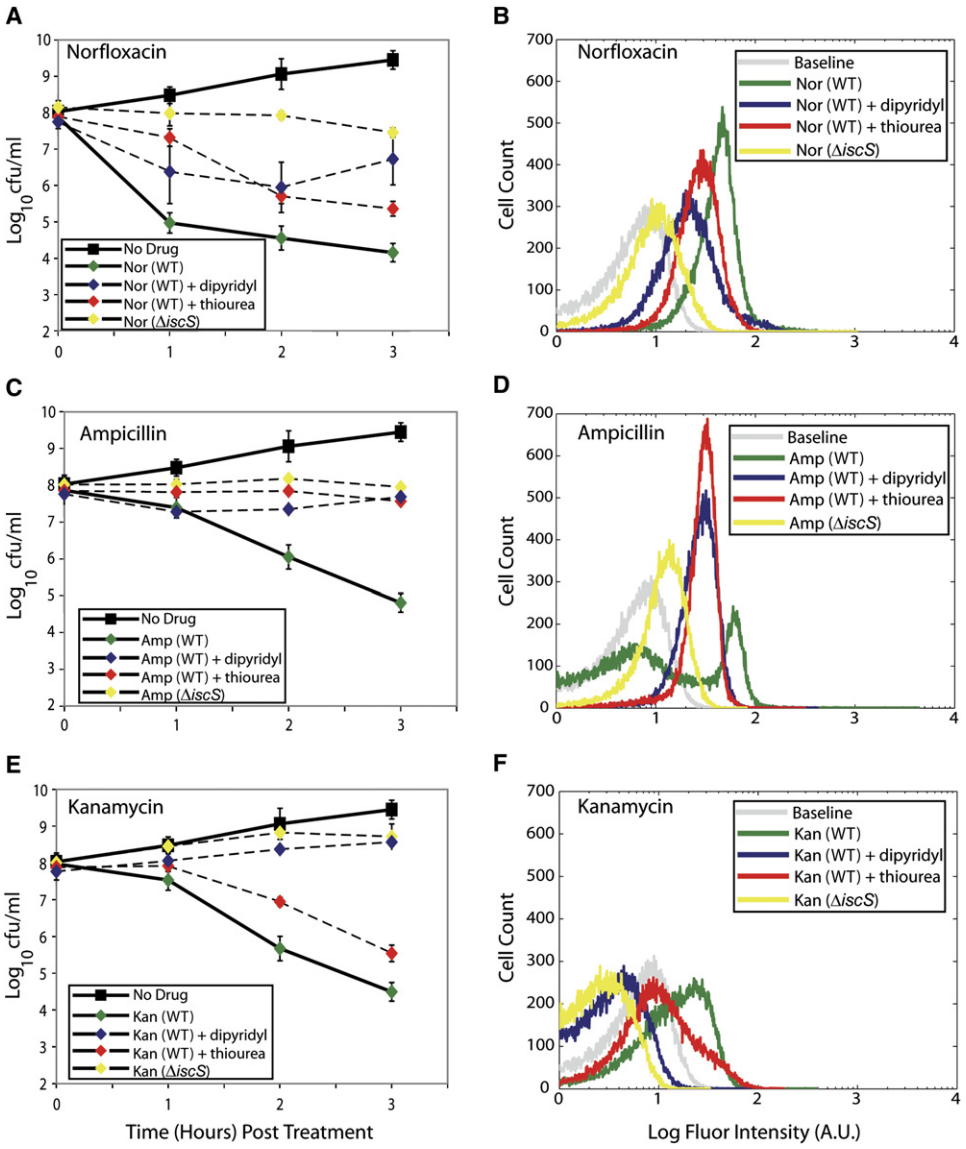

Figure 2. Effect of Iron Chelation, Hydroxyl Radical Quenching, and Disabling of Iron-Sulfur Cluster Synthesis on the Killing Efficiency of Bactericidal Antibiotics

(A, C, and E) Log change in cfu/ml following exposure to 250 ng/ml Nor (A), 5 μg/ml Amp (C), or 5 μg/ml Kan (E). Changes in cfu/ml following addition of 500 μM 2,2′-dipyidyl (blue diamonds) or 150 mM thiourea (red diamonds) to wild-type (WT) *E. coli* and an iron-sulfur cluster synthesis mutant, Δ*iscS* (yellow diamonds), are shown. In each panel, black squares represent a no-drug control and green diamonds represent wild-type *E. coli* exposed to drug alone.

(B, D, and F) Generation of hydroxyl radicals following exposure to 250 ng/ml Nor (B), 5 μg/ml Amp (D), or 5 μg/ml Kan (F). Representative measurements are shown and were taken 3 hr following addition of drug. The gray line represents time-zero baseline measurements, and the green line represents wild-type *E. coli* exposed to drug alone. Changes in hydroxyl radical formation following addition of 500 μM 2,2′-dipyidyl (blue line) or 150 mM thiourea (red line) to wild-type *E. coli* and an iron-sulfur cluster synthesis mutant, Δ*iscS* (yellow line), are shown.

death following kanamycin treatment (Figure 2E), which was reflected by the capacity of thiourea to reduce, but not eliminate, kanamycin-mediated hydroxyl radical formation (Figure 2F); this requires further investigation. Addition of the radical quencher to bacteriostatic drug-treated cultures had minimal effects on the growth-arresting properties of these bacteriostatic classes of drugs (Figure S4B).

Our results with 2,2′-dipyridyl and thiourea indicate that hydroxyl radical formation and the Fenton reaction play a critical role in effective killing by quinolones, β-lactams, and aminoglycosides. The ferrous iron required for hydroxyl radical formation could come from extracellular sources, such as iron import, or from intracellular sources, such as iron storage proteins or iron-sulfur clusters. To determine whether disabling iron import would reduce

bactericidal drug lethality, we examined the efficacy of bactericidal antibiotics in a Δ*tonB* strain. TonB is a required protein in the energy-dependent step of iron transport across the inner membrane of *E. coli* (Moeck and Coulton, 1998), and a *tonB* knockout has previously been shown to have a protective effect following exposure to oxidant stress exogenously induced via application of hydrogen peroxide (Touati et al., 1995). Our data show that removal of *tonB* provided no protective effect against norfloxacin-, kanamycin-, or ampicillin-mediated killing (Figure S5). This suggests that the import of external iron does not play a significant role in effecting killing by bactericidal drugs.

To determine whether oxidative damage of iron-sulfur clusters is a key source of ferrous iron driving hydroxyl radical formation for bactericidal drugs, we examined the killing properties of the bactericidal drugs in a Δ*iscS* strain; the *iscS* knockout has been shown to significantly impair iron-sulfur cluster synthesis capabilities and result in a decrease in iron-sulfur cluster abundance (Djaman et al., 2004; Schwartz et al., 2000). In this strain, we observed a significant reduction in cell death following treatment with norfloxacin (Figure 2A), ampicillin (Figure 2C), or kanamycin (Figure 2E). We found that the protective effect of Δ*iscS* is related to a reduction in hydroxyl radical formation following treatment with norfloxacin (Figure 2B), ampicillin (Figure 2D), or kanamycin (Figure 2F). These results imply that intracellular ferrous iron is a key source for Fenton-mediated hydroxyl radical formation by bactericidal drugs.

Catabolic NADH Depletion Is the Trigger for Hydroxyl Radical Formation

It is interesting to consider how functionally distinct bactericidal drugs commonly stimulate damage to iron-sulfur clusters. The established mechanism underlying leaching of iron from iron-sulfur clusters predominantly occurs via superoxide (Imlay, 2006; Keyer and Imlay, 1996; Liochev and Fridovich, 1999), and it is well accepted that the majority of superoxide generation in *E. coli* occurs through oxidation of the respiratory electron transport chain driven by oxygen and the conversion of NADH to NAD^+ (Imlay and Fridovich, 1991). We utilized gene expression microarrays and statistical analyses (see Experimental Procedures) to find sets of genes commonly upregulated or downregulated by the bactericidal drugs norfloxacin, ampicillin, and kanamycin relative to the bacteriostatic drug spectinomycin (Table 1). Interestingly, pathway enrichment (q value < 0.05) using Gene Ontology (Ashburner et al., 2000; Camon et al., 2004) found NADH-coupled electron transport (NADH dehydrogenase I) to be a key upregulated pathway common to all three bactericidal drug classes (Table 1).

We used a modified version (Leonardo et al., 1996) of the NAD^+ cycling assay developed by Bernofsky and Swan (1973) to monitor NAD^+ and NADH concentrations in wild-type *E. coli* following treatment with norfloxacin, ampicillin, and kanamycin (Figure 3A). For all three bactericidal drugs, we observed a >5-fold increase in the NAD^+/NADH ratio 0.5 hr after drug addition (Figure 3A). This ratio returned to untreated levels by 1 hr (Figure 3A). The increase in the NAD^+/NADH ratio was predominantly due to a large relative drop in NADH accompanied by a modest surge in NAD^+. This spike was not observed in an untreated culture, where the NAD^+/NADH ratio remained tightly bounded (Figure 3A). More importantly, treatment with the bacteriostatic drug spectinomycin had no effect on the NAD^+/NADH ratio relative to the untreated culture (Figure 3A). A surge in NADH consumption upon exposure to bactericidal antibiotics likely induces a burst in superoxide generation via the respiratory chain. Accordingly, these events may promote destabilization of iron-sulfur clusters, stimulation of the Fenton reaction, and cell death.

NADH is generated from NAD^+ during the TCA cycle (Cronan and Laporte, 2006). Therefore, loss of TCA-cycle component genes should reduce the available pool of NADH, decrease superoxide generation, and lead to increased survival following exposure to bactericidal drugs. Since NADH is produced at different points along the TCA cycle, the increase in survival should follow a gradient relative to the number of NADH molecules produced. Loss of genes before production of the first reduced dinucleotide (e.g., aconitase B [*acnB*] or isocitrate dehydrogenase [*icdA*]) should lead to larger increases in survival than loss of genes after the various NADH-producing steps in the TCA cycle (e.g., 2-ketoglutarate dehydrogenase [*sucB*, *sucA*, *lpdA*] or malate dehydrogenase [*mdh*]) (Figure 3B). We found that blocking the TCA cycle before the formation of the first reduced dinucleotide (Δ*icdA* and Δ*acnB*) led to increased survival following norfloxacin treatment, which had the largest increase in NAD^+/NADH ratio, whereas TCA-cycle knockouts after this point (Δ*sucB* and Δ*mdh*) behaved like wild-type (Figure 3C). Blocking the TCA cycle through to the second NADH formation step (Δ*acnB*, Δ*icdA*, and Δ*sucB*) led to increased survival following ampicillin treatment, while blocking the last NADH formation step (Δ*mdh*) did not affect survival (Figure 3D). Finally, each of the TCA-cycle knockout strains (Δ*acnB*, Δ*icdA*, Δ*sucB*, and Δ*mdh*) exhibited increased survival following exposure to kanamycin (Figure 3E).

It is important to note that aconitase A (AcnA) and aconitase B are the two main forms of aconitase in *E. coli*: AcnB functions as the main catabolic enzyme in the TCA cycle, while AcnA responds to oxidative stress (Cunningham et al., 1997). As expected, for all three classes of bactericidal drugs, we observed increased survival only with Δ*acnB*; Δ*acnA* behaved like wild-type (Figures 3C–3E). Interestingly, one of the first mutants selected for resistance to low levels of nalidixic acid, a quinolone, was mapped to a loss of isocitrate dehydrogenase (*icdA*) (Helling and Kukora, 1971), while later studies found that removing both *acnA* and *acnB* similarly conferred resistance (Gruer et al., 1997). The surge in NADH consumption induced by bactericidal drugs, coupled with the phenotypic results from the TCA-cycle knockouts, all point toward efficient

Table 1. Common Set of Differentially Expressed Genes for Bactericidal Antibiotics

Gene	Function
Upregulated (38)	
apaG	protein associated with Co^{2+} and Mg^{2+} efflux
arsC	arsenate reductase, drug/analog sensitivity
asnA	asparagine synthetase
b3275	23S ribosomal RNA of rrnD operon
cpxP	periplasmic protein combats stress, periplasmic repressor of cpx regulon by interaction with CpxA
dipZ	fused thiol:disulfide interchange protein, activator of DsbC
dnaK	chaperone Hsp70, cochaperone with DnaJ
groL	Cpn60 chaperonin GroEL, large subunit of GroESL
groS	Cpn10 chaperonin GroES, small subunit of GroESL
hdfR	transcriptional regulator of the flhDC operon
hslU	molecular chaperone and ATPase component of HslUV protease
murF	UDP-N-acetylmuramoyl-tripeptide:D-alanyl-D-alanine ligase
nuoC[a]	NADH:ubiquinone oxidoreductase, NADH dehydrogenase I chain C,D
nuoE[a]	NADH dehydrogenase subunit E, catalyzes the transfer of electrons from NADH to ubiquinone
nuoF[a]	NADH:ubiquinone oxidoreductase, NADH dehydrogenase I chain F
pdxA	NAD-dependent 4-hydroxy-L-threonine phosphate dehydrogenase
pepD	aminoacyl-histidine dipeptidase (peptidase D)
phnD	phosphonate/organophosphate ester transporter subunit
phoU	negative regulator of PhoR/PhoB two-component system, negative regulator for pho regulon and putative enzyme in phosphate metabolism
ppk	polyphosphate kinase, component of RNA degradosome
pstB	ATP-binding component of high-affinity phosphate-specific transport system
ptsA	PEP-protein phosphotransferase system enzyme I
ptsP	mannose-specific enzyme IIC component of PTS
rrsC	16S ribosomal RNA of rrnC operon
rrsG	16S ribosomal RNA of rrnG operon
rrsH	16S ribosomal RNA of rrnH operon
sbcD	ATP-dependent dsDNA exonuclease
tnaB	low-affinity tryptophan permease
xerC	site-specific tyrosine recombinase, affects chromosome segregation at cell division
ybeY	hypothetical protein
ybjH	hypothetical protein
ygdH	hypothetical protein
ygiB	conserved outer membrane protein
yhcM	conserved protein with nucleoside triphosphate hydrolase domain
yihQ	putative glycosidase
yihT	putative aldolase
yijO	predicted DNA-binding transcriptional regulator
yjbE	hypothetical protein
Downregulated (142)	
ade	purine ribonucleotide biosynthesis
aroM	protein of aro operon, regulated by aroR
b1229	predicted protamine-like protein
b1231	tRNA-Tyr
b2087	pseudogene, repressor for gat operon
bacA	putative transport, drug/analog sensitivity
blr	beta-lactam resistance membrane protein
cdd	salvage of nucleosides and nucleotides, cytidine deaminase
cdsA	fatty acid and phosphatidic acid biosynthesis
chpR	antitoxin of the ChpA-ChpR toxin-antitoxin system
cmr	proton motive force efflux pump
cobU	adenosylcobinamide kinase/ adenosylcobinamide-phosphate guanylyltransferase
csdA	cysteine sulfinate desulfinase
cspF	Qin prophage, cold-shock protein

Table 1. *Continued*

Gene	Function
dapE	succinyl-diaminopimelate desuccinylase
dusC	tRNA-dihydrouridine synthase C
exo	DNA exonuclease IX, 3′-phosphodiesterase activity at sites with 3′ incised apurinic/apyrimidinic sites, can remove 3′ phosphoglycolate groups
fruA	fructose-specific transport protein
fruB	fructose-specific IIA/fpr component
fruK	1-phosphofructokinase
gcvA	DNA-binding transcriptional dual regulator, positive regulator of gcv operon
gltS	glutamate transporter
gntK	gluconate kinase 2, gluconokinase 2
gntT	gluconate transporter, gluconate permease
gntU	gluconate transporter, low-affinity GNT 1 system
gpmB	phosphoglycerate mutase
idnK	D-gluconate kinase
insJ	IS150 protein InsA, transposon-related functions
insN-2	KpLE2 phage-like element, transposon-related functions
intB	KpLE2 phage-like element, predicted integrase
ispU	undecaprenyl pyrophosphate synthase
lpxC	UDP-3-O-acyl N-acetylglucosamine deacetylase
lpxL	lauryl-acyl carrier protein-dependent acyltransferase
lsrR	lsr operon transcriptional repressor
maa	maltose O-acetyltransferase
mdtI	multidrug efflux system transporter, possible chaperone
metN	DL-methionine transporter subunit
mltA	membrane-bound lytic murein transglycosylase A
molR	pseudogene molybdate metabolism regulator
nanA	N-acetylneuraminate lyase
norR	anaerobic nitric oxide reductase transcription regulator, required for the expression of anaerobic nitric oxide reductase

Table 1. *Continued*

Gene	Function
nudE	ADP-ribose diphosphatase
obgE	GTPase involved in cell partioning and DNA repair
pabC	4-amino-4-deoxychorismate lyase
priC	primosomal replication protein N″
puuA	putative glutamine synthetase
puuD	gamma-Glu-GABA hydrolase
puuR	DNA-binding transcriptional repressor
rdlA	antisense RNA, trans-acting regulator of ldrA translation
relB	bifunctional antitoxin of the RelE-RelB toxin-antitoxin system, transcriptional repressor
relE	toxin of the RelE-RelB toxin-antitoxin system
rem	predicted protein
renD	DLP12 prophage, predicted protein
rluC	23S rRNA pseudouridylate synthase
rpiB	ribose-5-phosphate isomerase B
rttR	rtT sRNA, processed from tyrT transcript, may modulate the stringent response
rumB	RNA uridine methyltransferase B
ruvB	Holliday junction DNA helicase B
rygC	sRNA, function unknown
sanA	transport, drug/analog sensitivity
sieB	Rac prophage
sirA	small protein required for cell growth, affects RpoS stability
tadA	tRNA-specific adenosine deaminase
torR	DNA-binding response regulator in two-component regulatory system with TorS
tyrP	tyrosine-specific transport system
yadR	hypothetical protein
yagI	predicted DNA-binding transcriptional regulator
yahA	predicted DNA-binding transcriptional regulator
ybcW	hypothetical protein
ybcY	predicted SAM-dependent methyltransferase
ybdH	predicted oxidoreductase
ybiN	predicted SAM-dependent methyltransferase

(*Continued on next page*)

Table 1. *Continued*

Gene	Function
ycbW	hypothetical protein
ycdC	predicted DNA-binding transcriptional regulator
ycdP	predicted inner membrane protein
ycdT	predicted diguanylate cyclase
ycdZ	predicted inner membrane protein
yceG	predicted aminodeoxychorismate lyase, putative thymidylate kinase
ycjM	predicted glucosyltransferase, putative polysaccharide hydrolase
ydgC	conserved inner membrane protein associated with alginate biosynthesis
ydgK	conserved inner membrane protein
ydhI	predicted inner membrane protein
ydjE	predicted transporter
ydjF	putative DEOR-type transcriptional regulator
ydjL	predicted oxidoreductase, Zn-dependent and NAD(P)-binding
ydjM	predicted inner membrane protein regulated by LexA
yeaS	neutral amino-acid efflux system
yebN	conserved inner membrane protein
yecF	hypothetical protein
yedV	putative two-component sensor protein
yegJ	hypothetical protein
yegQ	predicted peptidase
yegW	predicted DNA-binding transcriptional regulator
yegZ	pseudogene, gpD phage P2-like protein D
yeiS	predicted inner membrane protein
yejG	hypothetical protein
yfaZ	predicted outer membrane porin protein
yfbP	hypothetical protein
yfbV	hypothetical protein
yfeS	hypothetical protein
yfeU	N-acetylmuramic acid-6-phosphate etherase
yfeY	hypothetical protein
yfeZ	predicted inner membrane protein
yfgO	putative permease

Table 1. *Continued*

Gene	Function
yfhL	predicted 4Fe-4S cluster-containing protein
yfiF	predicted methyltransferase
ygdL	hypothetical protein
ygeP	hypothetical protein
ygeQ	hypothetical protein
yggN	hypothetical protein
ygiT	predicted DNA-binding transcriptional regulator
ygjM	predicted DNA-binding transcriptional regulator
ygjN	hypothetical protein
yhaM	hypothetical protein
yhaO	putative transport system permease protein
yhbE	conserved inner membrane protein
yhbP	hypothetical protein
yhdL	hypothetical protein
yhjQ	cell division protein (chromosome-partitioning ATPase) pseudogene
yiiX	predicted peptidoglycan peptidase
yjaA	hypothetical protein
yjaH	hypothetical protein
yjeJ	hypothetical protein
yjeM	predicted transporter
yjeO	conserved inner membrane protein
yjhB	putative transport protein
yjhC	predicted oxidoreductase, putative dehydrogenase
yjhE	predicted membrane protein (pseudogene)
yjhI	predicted DNA-binding transcriptional regulator
yjhP	putative methyltransferase
yjhQ	predicted acetyltransferase
yjhX	hypothetical protein
ykiA	hypothetical protein
ymcD	hypothetical protein
ynaK	hypothetical protein
ynbB	predicted CDP-diglyceride synthase, putative phosphatidate cytidyltransferase
ynjI	predicted inner membrane protein
yohL	hypothetical protein

Table 1. *Continued*

Gene	Function
ypeA	putative acetyltransferase
yraQ	predicted permease
yrhB	hypothetical protein
ytfA	predicted transcriptional regulator

[a] Pathway enrichment using Gene Ontology identified NADH-coupled electron transport (false discovery rate = 0.0345) as the only upregulated pathway common to all three bactericidal drug classes.

metabolism as an important aspect of killing by bactericidal drugs. This also suggests a mechanistic basis for the observation that carbon source limitation reduces the efficacy of killing by bactericidal drugs (Eng et al., 1991). Together, these results indicate that bactericidal drugs, for all of their diverse targets, stimulate hydroxyl radical formation through a common pathway.

All Bactericidal Drugs Induce DNA and Protein Damage

Hydroxyl radicals are extremely toxic and will readily damage proteins, membrane lipids, and DNA (Farr and Kogoma, 1991). Following application of bactericidal antibiotics, we would expect to see initiation of the DNA damage response system (SOS response), where RecA is activated by DNA damage, promoting autocleavage of the LexA repressor protein and stimulation of SOS response genes (Courcelle and Hanawalt, 2003; Friedberg et al., 2005). To examine SOS induction by the various bactericidal and bacteriostatic drugs used, we employed an engineered promoter-reporter gene construct that expresses green fluorescent protein (GFP) upon LexA autocleavage.

As expected, we observed a significant increase in SOS activity upon treatment with norfloxacin (Figure 4). β-lactams have recently been shown to induce expression of the SOS response mediator of filamentation, *sulA*, through the DpiBA two-component system (Miller et al., 2004).

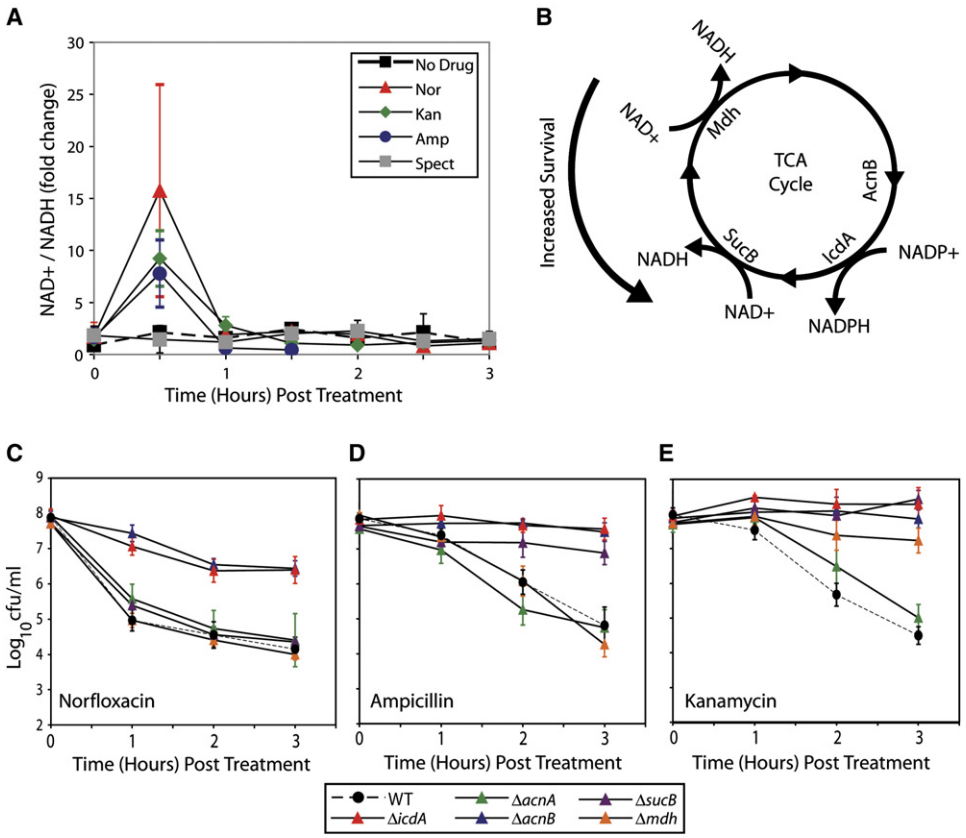

Figure 3. Role of the Tricarboxylic Acid Cycle and NAD$^+$/NADH in Bactericidal Antibiotic-Induced Cell Death

(A) Fold change in NAD$^+$/NADH (nmol/ml) following treatment with 250 ng/ml Nor (red triangles), 5 μg/ml Amp (blue circles), 5 μg/ml Kan (green diamonds), 400 mg/ml Spect (gray squares), or no drug (black squares, dashed line). NAD$^+$ and NADH were below the detection limit between 2 and 3 hr after the addition of ampicillin.

(B) Predicted increase in survival for tricarboxylic acid (TCA) cycle gene knockouts exposed to bactericidal drugs.

(C–E) Log change in cfu/ml. Survival of wild-type *E. coli* (black circles, dashed line), Δ*icdA* (red triangles), Δ*acnA* (green triangles), Δ*acnB* (blue triangles), Δ*sucB* (purple triangles), and Δ*mdh* (orange triangles) following treatment with 250 ng/ml Nor (C), 5 μg/ml Amp (D), and 5 μg/ml Kan (E).

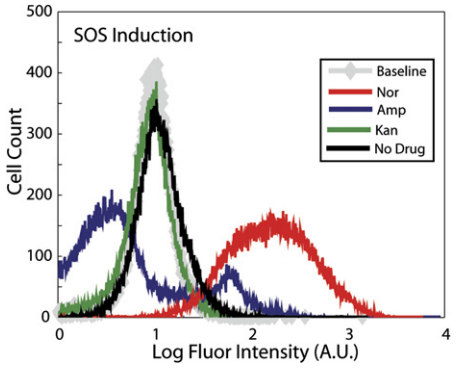

Figure 4. SOS Induction in *E. coli* by Bactericidal Antibiotics

Activation of the SOS (DNA damage) response was monitored using an engineered sensor construct that employs the LexA repressor for control of green fluorescent protein (GFP) expression. Representative GFP histogram measurements taken 3 hr after addition of bactericidal antibiotics (25 ng/ml Nor, red line; 5 μg/ml Amp, blue line; 5 μg/ml Kan, green line) are shown.

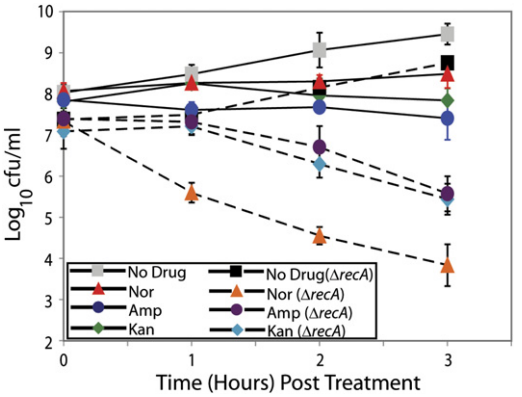

Figure 5. Potentiation of Bactericidal Antibiotics in Δ*recA E. coli*

Log change in cfu/ml of Δ*recA E. coli* following exposure to 25 ng/ml Nor (orange triangles), 2 μg/ml Amp (purple circles), and 3 μg/ml Kan (cyan diamonds). For comparison, cfu/ml are also shown for wild-type *E. coli* exposed to 25 ng/ml Nor (red triangles), 2 μg/ml Amp (blue circles), and 3 μg/ml kanamycin (green diamonds), as well as for no-drug controls (wild-type, gray squares; Δ*recA*, black squares). We used lower concentrations of Nor, Amp, and Kan in these experiments to highlight the significant increase in killing in a *recA* knockout.

LexA-driven GFP expression showed that ampicillin induced the SOS response via RecA activation (Figure 4), and the bimodal distribution is consistent with the observed bimodal distribution of hydroxyl radical formation following ampicillin treatment (Figure 1D). Following kanamycin treatment, we did not see any change in SOS activity over the course of the experiment (Figure 4). Since our reporter construct requires active transcription and translation to express GFP upon LexA autocleavage and kanamycin blocks translation, these data (Figure 4) do not rule out oxidative DNA damage following kanamycin treatment, particularly given our hydroxyl radical data (Figure 1D) and the damage that these oxidative radicals can cause to DNA.

Our results concerning hydroxyl radical formation (Figure 1D) provide a mechanistic basis for the earlier findings that the killing effects of quinolones (Lewin et al., 1989) and β-lactams (Miller et al., 2004) can be potentiated by knocking out *recA* and disabling the SOS response, which we confirmed as shown in Figure 5. To demonstrate that disabling the SOS response can also increase the potency of aminoglycosides, we examined kanamycin's killing efficiency in a *recA* knockout. We observed, in the Δ*recA* strain compared to wild-type, a significant increase in cell death following addition of kanamycin (Figure 5). The increased sensitivity of the Δ*recA* strain highlights the importance of an intact DNA damage repair system for mitigating the effects of hydroxyl radical-mediated DNA damage induced by all three major classes of bactericidal antibiotics (see Supplemental Data for results with bacteriostatic drugs). The increased sensitivity is most evident following norfloxacin treatment, where the primary DNA-damaging properties of quinolones are amplified by hydroxyl radical-mediated damage to DNA.

As noted above, hydroxyl radicals will also damage proteins and membrane lipids in addition to DNA. In our gene expression analysis comparing bactericidal to bacteriostatic antibiotic treatment (Table 1), we see significant upregulation of genes involved in the regulation of misfolded proteins (*hslU*, *dnaK*, *groL*, *groS*) as well as a negative regulator of a key stress-response system (*cpxP*) (Danese and Silhavy, 1998). This result is expected in the context of aminoglycosides, as protein mistranslation is one of the phenotypes separating aminoglycosides from bacteriostatic ribosome inhibitors (Davis, 1987; Weisblum and Davies, 1968). However, we see this response for all bactericidal drugs, including the DNA-damaging quinolones and cell-wall synthesis-inhibiting β-lactams. This suggests that in addition to hydroxyl radical-mediated DNA damage, there is enough hydroxyl radical-mediated protein damage to require activation of chaperone systems.

In addition to heat-shock genes, there are a number of genes involved in cell-wall and outer membrane turnover that are significantly upregulated (*pepD*, *murF*) or downregulated (*dapE*, *lpxC*, *lpxL*, *bacA*, *ispU*) by all three bactericidal antibiotics (Table 1). Gene expression changes among these cell envelope systems have been observed following oxidative damage with paraquat (Pomposiello et al., 2001). Further discussion of our gene expression analysis is provided in the Supplemental Data.

DISCUSSION

In this study, we have shown that the three major classes of bactericidal drugs all utilize a common mechanism of killing whereby they stimulate the production of lethal doses of hydroxyl radicals (Figure 6). We demonstrated through application of an iron chelator that quinolones,

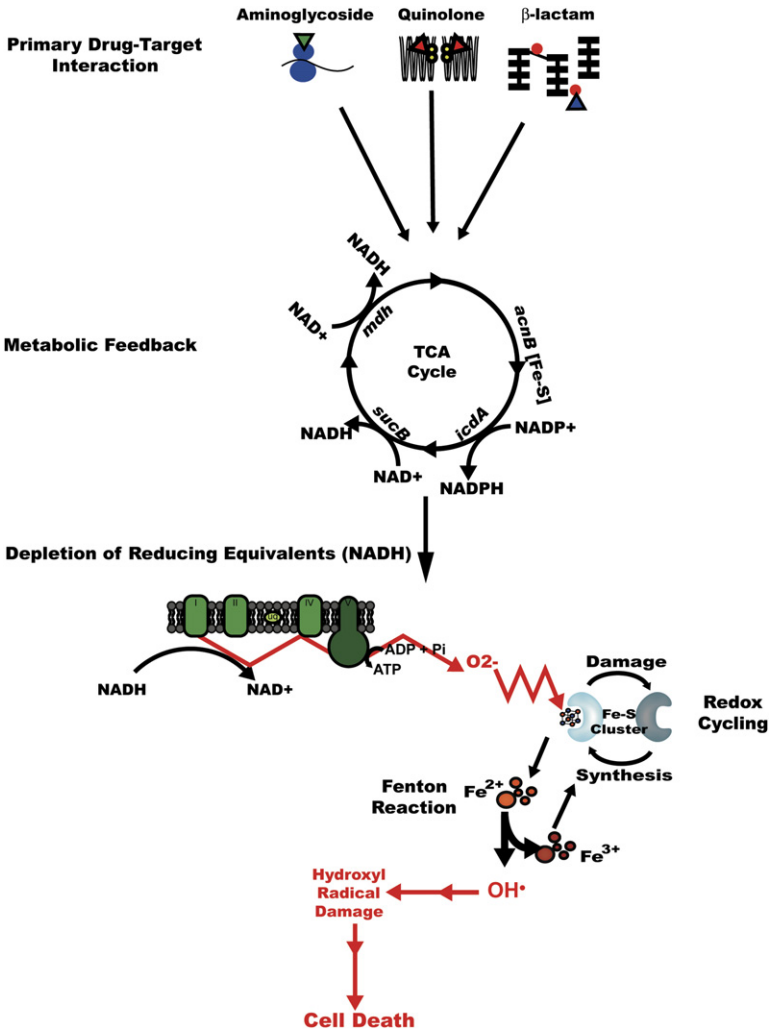

Figure 6. Proposed Model for Common Mechanism of Killing by Bactericidal Antibiotics

The primary drug-target interactions (aminoglycoside with the ribosome, quinolone with DNA gyrase, and β-lactam with penicillin-binding proteins) stimulate oxidation of NADH via the electron transport chain that is dependent upon the TCA cycle. Hyperactivation of the electron transport chain stimulates superoxide formation. Superoxide damages iron-sulfur clusters, making ferrous iron available for oxidation by the Fenton reaction. The Fenton reaction leads to hydroxyl radical formation, and the hydroxyl radicals damage DNA, proteins, and lipids, which results in cell death.

β-lactams, and aminoglycosides stimulate hydroxyl radical formation via the Fenton reaction. Importantly, both the iron chelator and a hydroxyl radical quencher attenuate killing by bactericidal drugs, suggesting that hydroxyl radicals contribute to bactericidal antibiotic-mediated cell death. While each of the bactericidal drugs tested have different primary drug-target interactions, we have shown they all converge on this free-radical-based common pathway via a metabolic response involving the TCA cycle that induces rapid depletion of NADH. We contend that this stimulates free-radical damage of iron-sulfur clusters, leading to destabilization or leaching of ferrous iron that participates in the Fenton reaction, ultimately resulting in hydroxyl radical formation and cell death (Figure 6). Using the *iscS* and *tonB* knockouts, we showed that intracellular iron-sulfur clusters are an important source of the iron required to stimulate Fenton-mediated hydroxyl radical formation.

Interestingly, previous in vitro work has shown that, due to their structures, bactericidal and bacteriostatic antibiotics can directly induce formation of reactive oxygen species particularly in the presence of excess transition metals such as copper or iron (Gutteridge et al., 1998), although some of these reactions have turned out to be of little likely consequence in vivo (Macomber et al., 2007). In this study, we showed in vivo that bactericidal, but not bacteriostatic, antibiotics stimulate the production of hydroxyl radicals (Figure 1). In addition, the coordinated metabolic and genetic changes we identified (Figure 3), along with our gene expression results comparing bactericidal to bacteriostatic drug treatment (Table 1), suggest that a specific series of intracellular events accompanying the primary mode of action of bactericidal antibiotics are responsible for the generation of lethal levels of hydroxyl radicals (Figure 6). As noted above, we showed that all bactericidal drug classes utilize internal iron from iron-sulfur clusters to promote Fenton-mediated hydroxyl radical formation and that these events appear to be mediated by the TCA cycle and a transient depletion of NADH.

It is somewhat surprising that current bactericidal antibiotics do not target the TCA cycle or respiratory chain

more often, yet there is evidence that some mechanisms of resistance to bactericidal drugs occur via these pathways. Aminoglycoside uptake and lethality are associated with mistranslation, functional ubiquinones, a working electron transport chain, and oxidative phosphorylation (Taber et al., 1987). Among quinolones, one of the original nalidixic acid-resistant strains was mapped to a loss of isocitrate dehydrogenase, and a similar effect was observed following removal of aconitase B (Gruer et al., 1997; Helling and Kukora, 1971). Also, the efficacy of quinolones in stationary phase can be enhanced by adding oxygen to a stationary-phase culture (Morrissey and Smith, 1994), and recent evidence suggests that metabolic activity and oxygen tension are important indicators of quinolone activity against biofilms (Walters et al., 2003). This suggests that targeted inhibition of the TCA cycle or electron transport chain may lead to loss of metabolic activity and increased bactericidal drug resistance, rather than a hyperactive metabolic state leading to an increase in bactericidal drug sensitivity.

Other pathways besides the TCA cycle are likely involved in regulating and responding to bactericidal antibiotic-mediated effects and deserve further study. For example, further exploration of the posttranscriptional relationship among iron, metabolism, and iron-sulfur cluster-containing proteins (Hantke, 2001) is needed to identify any posttranscriptional events not captured by gene expression analysis that coordinate or trigger this common cell death pathway. Importantly, our gene expression results (Table 1) suggest that all bactericidal antibiotics induce protective responses to reactive oxygen species. There is a well-established regulatory overlap between the genetic responses to oxidative stress and antibiotic exposure: the multidrug efflux pump *acrAB* is regulated by the superoxide-sensitive SoxR system, and it has been suggested that the *soxR*-regulated genes represent a coordinated response against antibiotics (Greenberg et al., 1990). These response systems to reactive oxygen species may represent pathways that can be targeted to enhance the efficacy of current bactericidal antibiotics. In addition, elucidation of the steps that occur after the diverse bactericidal drug-target interactions but before the step of NADH depletion is needed to further our understanding of the common mechanism of killing shown in Figure 6.

Antibacterial drug design has focused on blocking essential cellular functions (Walsh, 2003). This has yielded significant advances in antibacterial therapy; however, the ever-increasing prevalence of antibiotic-resistant strains has made it critical that we develop novel, more effective means of killing bacteria. Our results indicate that targeting bacterial systems that remediate hydroxyl radical damage, including proteins involved in triggering the DNA damage response, e.g., RecA, is a viable means of potentiating all three major classes of bactericidal drugs. Moreover, pathway analyses and systems biology approaches may uncover druggable targets for stimulating hydroxyl radical formation, which could result in new classes of bactericidal antibiotics.

EXPERIMENTAL PROCEDURES

Media and Antibiotics

All experiments were performed in Luria-Bertani (LB) medium (Fisher Scientific). For bactericidal drug experiments in *E. coli*, we used the antibiotics ampicillin (Fisher Scientific), kanamycin (Fisher Scientific), and norfloxacin (Sigma). For experiments in *S. aureus*, we used norfloxacin and vancomycin (Teknova). For bacteriostatic drug experiments in *E. coli*, we used the antibiotics rifamycin SV (MP Biomedicals), chloramphenicol (Acros Organics), tetracycline (MP Biomedicals), erythromycin (Sigma), and spectinomycin (MP Biomedicals). For experiments in *S. aureus*, we used chloramphenicol.

Strains

All *E. coli* experiments were performed with MG1655 (ATCC 700926)-derived strains (Table S4). The *recA*, *iscS*, and TCA-cycle knockouts were constructed using P1 phage transduction and were derived from an *E. coli* single-gene knockout library (Baba et al., 2006) (Table S4). Positive P1 transductants were confirmed by acquisition of kanamycin resistance and PCR. Removal of the kanamycin-resistance cassette was accomplished using the pcp20 plasmid (Datsenko and Wanner, 2000) (Table S4) and confirmed by PCR prior to experimentation. For work with *S. aureus*, we used a *S. aureus* subspecies *aureus* Rosenbach (Table S4) strain obtained from ATCC (29740).

Growth Conditions

In our experiments, we compared the growth and survival of untreated exponential-phase *E. coli* or *S. aureus* to cultures treated with the above antibiotics at given concentrations. Briefly, cultures were grown in 25 ml LB medium in 250 ml flasks and incubated at 37°C and 300 rpm, and antibiotics were added at early exponential phase. To ensure that light-induced redox cycling of antibiotics (Martin et al., 1987; Umezawa et al., 1997) was not a confounding factor, all experiments were performed in light-insulated shakers. For the iron chelation experiments, 2,2′-dipyridyl (500 μM, Sigma) was added simultaneously with antibiotics. For the hydroxyl radical quenching experiments, thiourea (150 mM, Fluka) was added simultaneously with antibiotics. See Supplemental Data for more details.

DNA Damage Sensor and Hydroxyl Radical Experiments Using Flow Cytometry

To monitor the occurrence of DNA damage, we employed an engineered DNA damage sensor construct (see Supplemental Data). All data were collected using a Becton Dickinson FACSCalibur flow cytometer with a 488 nm argon laser and a 515–545 nm emission filter (FL1) at low flow rate. At least 50,000 cells were collected for each sample. The following photomultiplier tube (PMT) voltage settings were used: E00 (FSC), 360 (SSC), and 700 (FL1). To detect hydroxyl radical formation, we used the fluorescent reporter dye 3′-(p-hydroxyphenyl) fluorescein (HPF, Invitrogen) at a concentration of 5 μM. The following PMT voltage settings were used: E00 (FSC), 360 (SSC), and 825 (FL1). Calibrite beads (Becton Dickinson) were used for instrument calibration. Flow data were processed and analyzed with MATLAB (The MathWorks). In all experiments, cells were grown as described above. Samples were taken immediately before addition of drug (time zero) and then every hour for 3 hr. At each time point, approximately 10^6 cells were collected, washed once, and resuspended in filtered 1× PBS (pH 7.2) (Fisher Scientific) prior to measurement.

NAD^+/NADH Extraction and NAD Cycling Assay

Dinucleotide extraction and the NAD cycling assay were performed as previously described (Leonardo et al., 1996). See Supplemental Data for more details.

Gene Expression Analysis

We compared the microarray-determined mRNA profiles (Affymetrix *E. coli* Antisense2 genome arrays) of wild-type *E. coli* cultures in response to bactericidal antibiotic treatment (250 ng/ml norfloxacin, 5 μg/ml ampicillin, and 5 μg/ml kanamycin) to that of bacteriostatic antibiotic treatment (400 μg/ml spectinomycin) or untreated cells. For all experiments, overnight cultures were diluted 1:500 into 250 ml LB medium in 1 l flasks for collection of total RNA. Early exponential-phase cultures were split (50 ml LB medium into 5× 250 ml flasks), and antibiotics were added as described above. Samples for microarray analysis were taken immediately before treatment (time zero) and then at 30, 60, and 120 min posttreatment. RNA collection and microarray processing are described further in the Supplemental Data.

The resulting microarray *.CEL files were combined with *.CEL files from arrays that comprise the M^{3D} compendium (Faith et al., 2007) (http://m3d.bu.edu; E_coli_v3_Build_3) and RMA normalized (Bolstad et al., 2003) with RMAExpress, for a total of 524 RMA-normalized *E. coli* expression arrays. Each gene's standard deviation of expression, σ, was calculated and used to construct the z scale difference between that gene's normalized expression in a given experimental condition (bactericidal drug treatment) versus a control (bacteriostatic drug treatment):

$$\Delta z_{exp} = \frac{X_{exp} - X_{ctl}}{\sigma}.$$

This allowed us to measure each gene's change in expression for a given experiment in units of standard deviation, a form of the z test. For each time point in each bactericidal experiment set (norfloxacin, ampicillin, and kanamycin), we converted Δz scores to p values and chose significantly up- and downregulated genes by selecting those with a q value < 0.05 (false discovery rate) (Storey and Tibshirani, 2003). We merged the resultant gene lists across all time points (set union) to obtain a coarse profile of the difference in expression between a given bactericidal drug and spectinomycin. Finally, we determined the common set of all genes that were up- or downregulated by bactericidal concentrations of norfloxacin, kanamycin, and ampicillin with respect to spectinomycin (three-way set intersect). For additional pathway-level insights, we performed Gene Ontology-based enrichment (Ashburner et al., 2000; Camon et al., 2004) of the up- and downregulated gene lists using GO::TermFinder (Boyle et al., 2004), requiring pathway enrichment q values to be <0.05 and setting the p value estimation mode to bootstrapping.

Supplemental Data

Supplemental Data include Supplemental Discussion, Supplemental Experimental Procedures, Supplemental References, ten figures, and four tables and can be found with this article online at http://www.cell.com/cgi/content/full/130/5/797/DC1/.

ACKNOWLEDGMENTS

We thank T. Gardner for the use of BL2 facilities for the *S. aureus* experiments; N. Gerry for processing the microarrays; M. Driscoll and J. Faith for an updated annotation of the Affymetrix Antisense2 microarray and maintaining the M^{3D} database; and M. Koeris, M. Driscoll, and N. Guido for comments on the manuscript. This work was supported by the National Science Foundation FIBR and Department of Energy GTL programs and NSF award EMSW21-RTG to J.J.C. J.J.C. is a founding member and minority shareholder of Cellicon Biotechnologies, Inc., an antibiotic discovery company.

Received: February 21, 2007
Revised: May 18, 2007
Accepted: June 27, 2007
Published: September 6, 2007

REFERENCES

Ashburner, M., Ball, C.A., Blake, J.A., Botstein, D., Butler, H., Cherry, J.M., Davis, A.P., Dolinski, K., Dwight, S.S., Eppig, J.T., et al. (2000). Gene ontology: tool for the unification of biology. The Gene Ontology Consortium. Nat. Genet. *25*, 25–29.

Baba, T., Ara, T., Hasegawa, M., Takai, Y., Okumura, Y., Baba, M., Datsenko, K.A., Tomita, M., Wanner, B.L., and Mori, H. (2006). Construction of Escherichia coli K-12 in-frame, single-gene knockout mutants: the Keio collection. Mol. Syst. Biol. *2*, 2006.0008.

Bernofsky, C., and Swan, M. (1973). An improved cycling assay for nicotinamide adenine dinucleotide. Anal. Biochem. *53*, 452–458.

Bolstad, B.M., Irizarry, R.A., Astrand, M., and Speed, T.P. (2003). A comparison of normalization methods for high density oligonucleotide array data based on variance and bias. Bioinformatics *19*, 185–193.

Boyle, E.I., Weng, S., Gollub, J., Jin, H., Botstein, D., Cherry, J.M., and Sherlock, G. (2004). GO::TermFinder–open source software for accessing Gene Ontology information and finding significantly enriched Gene Ontology terms associated with a list of genes. Bioinformatics *20*, 3710–3715.

Camon, E., Magrane, M., Barrell, D., Lee, V., Dimmer, E., Maslen, J., Binns, D., Harte, N., Lopez, R., and Apweiler, R. (2004). The Gene Ontology Annotation (GOA) Database: sharing knowledge in Uniprot with Gene Ontology. Nucleic Acids Res. *32*, D262–D266.

Chopra, I., and Roberts, M. (2001). Tetracycline antibiotics: mode of action, applications, molecular biology, and epidemiology of bacterial resistance. Microbiol. Mol. Biol. Rev. *65*, 232–260.

Courcelle, J., and Hanawalt, P.C. (2003). RecA-dependent recovery of arrested DNA replication forks. Annu. Rev. Genet. *37*, 611–646.

Cronan, J.E., Jr., and Laporte, D. (2006). Tricarboxylic acid cycle and glyoxylate bypass. In *Escherichia coli* and *Salmonella*: Cellular and Molecular Biology, A. Böck, R. Curtis, III, J.B. Kaper, F.C. Neidhardt, T. Nyström, K.E. Rudd, and C.L. Squires, eds. (Washington, DC: ASM Press). (http://www.ecosal.org/ecosal/modules/index.jsp?3.5.2).

Cunningham, L., Gruer, M.J., and Guest, J.R. (1997). Transcriptional regulation of the aconitase genes (acnA and acnB) of Escherichia coli. Microbiology *143*, 3795–3805.

Danese, P.N., and Silhavy, T.J. (1998). CpxP, a stress-combative member of the Cpx regulon. J. Bacteriol. *180*, 831–839.

Datsenko, K.A., and Wanner, B.L. (2000). One-step inactivation of chromosomal genes in Escherichia coli K-12 using PCR products. Proc. Natl. Acad. Sci. USA *97*, 6640–6645.

Davis, B.D. (1987). Mechanism of bactericidal action of aminoglycosides. Microbiol. Rev. *51*, 341–350.

Djaman, O., Outten, F.W., and Imlay, J.A. (2004). Repair of oxidized iron-sulfur clusters in Escherichia coli. J. Biol. Chem. *279*, 44590–44599.

Drlica, K., and Zhao, X. (1997). DNA gyrase, topoisomerase IV, and the 4-quinolones. Microbiol. Mol. Biol. Rev. *61*, 377–392.

Dwyer, D.J., Kohanski, M.A., Hayete, B., and Collins, J.J. (2007). Gyrase inhibitors induce an oxidative damage cellular death pathway in Escherichia coli. Mol. Syst. Biol. *3*, 91.

Eng, R.H., Padberg, F.T., Smith, S.M., Tan, E.N., and Cherubin, C.E. (1991). Bactericidal effects of antibiotics on slowly growing and nongrowing bacteria. Antimicrob. Agents Chemother. *35*, 1824–1828.

Faith, J.J., Hayete, B., Thaden, J.T., Mogno, I., Wierzbowski, J., Cottarel, G., Kasif, S., Collins, J.J., and Gardner, T.S. (2007). Large-scale mapping and validation of Escherichia coli transcriptional regulation from a compendium of expression profiles. PLoS Biol. *5*, e8.

Farr, S.B., and Kogoma, T. (1991). Oxidative stress responses in Escherichia coli and Salmonella typhimurium. Microbiol. Rev. *55*, 561–585.

Friedberg, E.C., Walker, G.C., Siede, W., Wood, R.D., Schultz, R.A., and Ellenberger, T. (2005). DNA Repair and Mutagenesis, Second Edition (Herndon, VA: ASM Press).

Greenberg, J.T., Monach, P., Chou, J.H., Josephy, P.D., and Demple, B. (1990). Positive control of a global antioxidant defense regulon activated by superoxide-generating agents in Escherichia coli. Proc. Natl. Acad. Sci. USA *87*, 6181–6185.

Gruer, M.J., Bradbury, A.J., and Guest, J.R. (1997). Construction and properties of aconitase mutants of Escherichia coli. Microbiology *143*, 1837–1846.

Gutteridge, J.M., Quinlan, G.J., and Kovacic, P. (1998). Phagomimetic action of antimicrobial agents. Free Radic. Res. *28*, 1–14.

Hantke, K. (2001). Iron and metal regulation in bacteria. Curr. Opin. Microbiol. *4*, 172–177.

Helling, R.B., and Kukora, J.S. (1971). Nalidixic acd-resistant mutants of Escherichia coli deficient in isocitrate dehydrogenase. J. Bacteriol. *105*, 1224–1226.

Imlay, J.A. (2006). Iron-sulphur clusters and the problem with oxygen. Mol. Microbiol. *59*, 1073–1082.

Imlay, J.A., and Linn, S. (1986). Bimodal pattern of killing of DNA-repair-defective or anoxically grown Escherichia coli by hydrogen peroxide. J. Bacteriol. *166*, 519–527.

Imlay, J.A., and Fridovich, I. (1991). Assay of metabolic superoxide production in Escherichia coli. J. Biol. Chem. *266*, 6957–6965.

Imlay, J.A., Chin, S.M., and Linn, S. (1988). Toxic DNA damage by hydrogen peroxide through the Fenton reaction in vivo and in vitro. Science *240*, 640–642.

Keyer, K., and Imlay, J.A. (1996). Superoxide accelerates DNA damage by elevating free-iron levels. Proc. Natl. Acad. Sci. USA *93*, 13635–13640.

Leonardo, M.R., Dailly, Y., and Clark, D.P. (1996). Role of NAD in regulating the adhE gene of Escherichia coli. J. Bacteriol. *178*, 6013–6018.

Lewin, C.S., Howard, B.M., Ratcliffe, N.T., and Smith, J.T. (1989). 4-quinolones and the SOS response. J. Med. Microbiol. *29*, 139–144.

Lewis, K. (2000). Programmed death in bacteria. Microbiol. Mol. Biol. Rev. *64*, 503–514.

Liochev, S.I., and Fridovich, I. (1999). Superoxide and iron: partners in crime. IUBMB Life *48*, 157–161.

Macomber, L., Rensing, C., and Imlay, J.A. (2007). Intracellular copper does not catalyze the formation of oxidative DNA damage in Escherichia coli. J. Bacteriol. *189*, 1616–1626.

Martin, J.P., Jr., Colina, K., and Logsdon, N. (1987). Role of oxygen radicals in the phototoxicity of tetracyclines toward Escherichia coli B. J. Bacteriol. *169*, 2516–2522.

Miller, C., Thomsen, L.E., Gaggero, C., Mosseri, R., Ingmer, H., and Cohen, S.N. (2004). SOS response induction by beta-lactams and bacterial defense against antibiotic lethality. Science *305*, 1629–1631.

Moeck, G.S., and Coulton, J.W. (1998). TonB-dependent iron acquisition: mechanisms of siderophore-mediated active transport. Mol. Microbiol. *28*, 675–681.

Morrissey, I., and Smith, J.T. (1994). The importance of oxygen in the killing of bacteria by ofloxacin and ciprofloxacin. Microbios *79*, 43–53.

Novogrodsky, A., Ravid, A., Rubin, A.L., and Stenzel, K.H. (1982). Hydroxyl radical scavengers inhibit lymphocyte mitogenesis. Proc. Natl. Acad. Sci. USA *79*, 1171–1174.

Pankey, G.A., and Sabath, L.D. (2004). Clinical relevance of bacteriostatic versus bactericidal mechanisms of action in the treatment of Gram-positive bacterial infections. Clin. Infect. Dis. *38*, 864–870.

Poehlsgaard, J., and Douthwaite, S. (2005). The bacterial ribosome as a target for antibiotics. Nat. Rev. Microbiol. *3*, 870–881.

Pomposiello, P.J., Bennik, M.H., and Demple, B. (2001). Genome-wide transcriptional profiling of the Escherichia coli responses to superoxide stress and sodium salicylate. J. Bacteriol. *183*, 3890–3902.

Repine, J.E., Fox, R.B., and Berger, E.M. (1981). Hydrogen peroxide kills Staphylococcus aureus by reacting with staphylococcal iron to form hydroxyl radical. J. Biol. Chem. *256*, 7094–7096.

Reynolds, P.E. (1989). Structure, biochemistry and mechanism of action of glycopeptide antibiotics. Eur. J. Clin. Microbiol. Infect. Dis. *8*, 943–950.

Schwartz, C.J., Djaman, O., Imlay, J.A., and Kiley, P.J. (2000). The cysteine desulfurase, IscS, has a major role in in vivo Fe-S cluster formation in Escherichia coli. Proc. Natl. Acad. Sci. USA *97*, 9009–9014.

Setsukinai, K., Urano, Y., Kakinuma, K., Majima, H.J., and Nagano, T. (2003). Development of novel fluorescence probes that can reliably detect reactive oxygen species and distinguish specific species. J. Biol. Chem. *278*, 3170–3175.

Storey, J.D., and Tibshirani, R. (2003). Statistical significance for genomewide studies. Proc. Natl. Acad. Sci. USA *100*, 9440–9445.

Taber, H.W., Mueller, J.P., Miller, P.F., and Arrow, A.S. (1987). Bacterial uptake of aminoglycoside antibiotics. Microbiol. Rev. *51*, 439–457.

Tenson, T., Lovmar, M., and Ehrenberg, M. (2003). The mechanism of action of macrolides, lincosamides and streptogramin B reveals the nascent peptide exit path in the ribosome. J. Mol. Biol. *330*, 1005–1014.

Tomasz, A. (1979). The mechanism of the irreversible antimicrobial effects of penicillins: how the beta-lactam antibiotics kill and lyse bacteria. Annu. Rev. Microbiol. *33*, 113–137.

Touati, D., Jacques, M., Tardat, B., Bouchard, L., and Despied, S. (1995). Lethal oxidative damage and mutagenesis are generated by iron in delta fur mutants of Escherichia coli: protective role of superoxide dismutase. J. Bacteriol. *177*, 2305–2314.

Umezawa, N., Arakane, K., Ryu, A., Mashiko, S., Hirobe, M., and Nagano, T. (1997). Participation of reactive oxygen species in phototoxicity induced by quinolone antibacterial agents. Arch. Biochem. Biophys. *342*, 275–281.

Walsh, C. (2000). Molecular mechanisms that confer antibacterial drug resistance. Nature *406*, 775–781.

Walsh, C. (2003). Where will new antibiotics come from? Nat. Rev. Microbiol. *1*, 65–70.

Walters, M.C., 3rd, Roe, F., Bugnicourt, A., Franklin, M.J., and Stewart, P.S. (2003). Contributions of antibiotic penetration, oxygen limitation, and low metabolic activity to tolerance of Pseudomonas aeruginosa biofilms to ciprofloxacin and tobramycin. Antimicrob. Agents Chemother. *47*, 317–323.

Wehrli, W., and Staehelin, M. (1971). Actions of the rifamycins. Bacteriol. Rev. *35*, 290–309.

Weisblum, B., and Davies, J. (1968). Antibiotic inhibitors of the bacterial ribosome. Bacteriol. Rev. *32*, 493–528.